

Elastic moduli of living epithelial pancreatic cancer cells and their skeletonized keratin intermediate filament network*

Nadine Walter and Tobias Busch

Max Planck Institute for Intelligent Systems, Heisenbergstr.3, D-70569 Stuttgart, Germany and Biophysical Chemistry, Institute for Physical Chemistry, University of Heidelberg, INF 253, D-69120 Heidelberg, Germany

Thomas Seufferlein

Department of Internal Medicine I, Martin-Luther-University Halle-Wittenberg, Ernst Grube Str. 40, D-01620 Halle, Germany

Joachim P. Spatz^{a)}

Max Planck Institute for Metals Research, Heisenbergstr.3, D-70569 Stuttgart, Germany & Biophysical Chemistry, Institute for Physical Chemistry, University of Heidelberg, INF 253, 69120 Heidelberg, Germany

(Received 31 March 2011; accepted 24 May 2011; published 1 July 2011)

In simple epithelia, such as living epithelial pancreatic cancer cells (Panc-1), unusual amounts of keratin filaments can be found, which makes these cells an ideal model system to study the role of keratin for cell mechanical properties. In this work, the elastic moduli of Panc-1 cells and their extracted *in-situ* subcellular keratin intermediate filament network are determined and compared with each other. For this, the living adherent cells and their extracted keratin network were probed with local quasistatic indentation testing during large deformations using the Atomic Force Microscope (AFM). We determined the elastic modulus of the skeletonized but structurally intact keratin network to be in the order of 10 Pa, while the living cell elastic modulus ranged from 100 to 500 Pa. By removing microfilaments, microtubules, membranes and soluble cytoplasmic components during keratin network extraction, we excluded effects caused by crosslinking with other filamentous fibers and from the viscosity of the cytoplasm. Thus, the determined elastic modulus equals the actual elastic modulus inherent to such a keratin filamentous network. In our assessment of the effective mechanical contribution of the architecturally intact, skeletonized keratin network to living cell mechanics, we come to the conclusion that it plays only a very limited role. Evidently, the quantitative dominance of keratin in these cells does not reflect a strong influence on determining the cell's elastic modulus. Instead, keratin like other filamentous structures in the cell's scaffolding, e.g., F-actin and microtubuli, is one part of a greater whole. © 2011 American Vacuum Society. [DOI: 10.1116/1.3601755]

I. INTRODUCTION

Cell mechanical properties define the ability of cells to resist physiologically relevant deformations and stresses that cells have to sustain inside the body. These properties also enable cells to perform specific tasks such as metastasis. To what extent different cell substructures, such as the different filamentous polymers of the cytoskeleton, contribute to the whole cell mechanical response on different time scales and deformation states, has yet to be fully investigated. While the role of the actin fiber cytoskeleton, which is present in all eukaryotic cells, has been studied in some detail, the mechanics and functions of the intermediate filament networks remain under-researched.

Cell mechanics seeks to understand the mechanical responses of whole cells to forces and deformations and the significance of individual cellular subcomponents for the mechanical behavior of the cell. Generally, if cells were not highly complex and dynamic units containing a multitude of

different substructures, measurements of cell mechanics would simply reflect the properties of cell stiffness and viscoelasticity. To measure and describe the biomechanical properties of cells, a wide range of probing techniques and biomimetic models have been developed.^{1,2} Several bulk homogenous material models have been proposed that describe the biophysical properties of cells depending on the cell type and probing method: linear elasticity, linear viscoelasticity and poroelasticity. A consequence of applying different experimental techniques and models when determining the cell mechanical properties is the creation of probing artifacts that result in a large range of experimentally determined mechanical constants for cells.

As the material response of a cell mainly depends on the fibrous cytoskeleton,³ cell mechanics focuses on the investigation of the different cytoskeletal networks, namely actin filaments, microtubules and intermediate filaments. Each type of filament is made from different protein subunits, which are cross-linked and bundled into fibers, which in turn are connected by associated proteins, such as the cytolinker plectin and the keratin bundling protein filaggrin.⁴⁻⁶ Addi-

*No proof corrections received from author prior to publication.

^{a)}Electronic mail: spatz@is.mpg.de

tionally, recent work shows that divalent ions can act as crosslinkers via electrostatic interaction in intermediate filament networks.⁷

Because the direct *in vivo* measurement of network properties is corrupted by other cellular structures, studies have been limited to investigating the properties of biomimetic filament suspensions and single fiber characteristics.⁷⁻¹⁰ Fiber properties, such as thickness and bending stiffness, which describe the resistance of the fibers to bend if a torque is applied, are known for actin, microtubules and intermediate filaments.¹¹ Microtubules are the thickest and straightest fibers inside the cell, with a diameter of 25 nm and a bending stiffness of 2.6×10^{-23} Nm². Actin filaments have a diameter of 8 nm and a bending stiffness of 7×10^{-26} Nm². Intermediate filaments have a diameter of about 10 nm and the lowest bending stiffness of only 4 to 12×10^{-27} Nm². The properties of the overall cytoskeletal network arise from a combination of single fiber properties and their structural assembly. Janmey *et al.*⁹ performed rheologic measurements on purified and repolymerized actin, vimentin and microtubules and performed direct comparisons between the different filaments at identical concentrations. It was found that actin filaments have a higher rigidity than intermediate filaments, but fluidize at high strains. In contrast, intermediate filaments exhibit strain hardening at high tensile strains without rupture.^{7,9,12}

Every cell type is composed of different types and amounts of specific cytoskeleton fibers. Simple epithelia, such as the pancreatic cancer cells we investigated here, have a well-developed keratin intermediate filament network in addition to actin and microtubules. It has been speculated that their keratin network may determine the main cell mechanical resistance to deformation in these cells.¹³

In accordance with semiflexible polymer physics, Yamada *et al.*⁸ found that for keratin intermediate filament suspensions bulk elasticity depends on both the polymer concentration as well as the polymer size. Vimentin and neurofilaments, both a subgroup of intermediate filaments, also show strong non-linear strain stiffening and predominantly elastic behavior, in agreement with the semiflexible polymer theory.⁷

Sivaramakrishnan *et al.*¹⁴ similarly found the materials response of the keratin intermediate filament network to be mainly elastic. In their study they measured the storage modulus, which determines the elastically stored energy of the *in-situ* keratin intermediate filament network extracted from alveolar epithelial cells with microrheological particle tracking. They showed that, same as in semiflexible polymers, the storage modulus increased with network density. Measurements at 1Hz yielded storage modulus values ranging from 95 to 335 dyn/cm², which translates into an elastic modulus of 30 to 110 Pa assuming a Poisson ratio of 0.5.

In the work presented in this publication we perform a direct comparison of the elastic moduli of living cells and their *in-situ* intermediate filament networks to clarify the role that keratin plays during deformation of cancerous epithelial cells. The elastic modulus of a living cell results from the

combined effects of numerous cellular components working together. By applying the same methodology and material model for both measurements, we are able to selectively extract and define the role of our chosen cytoskeleton constituent: the keratin filamentous network.

II. MATERIALS AND METHODS

A. Panc-1 cell culture, transfection and sample preparation

Panc-1 cells were kept in culture up to 70% confluency at 37 °C, in a 5% CO₂ atmosphere and DMEM cell medium (Gibco) supplemented with 10% fetal calf serum, FCS (PAA Laboratories), 1% Penicillin-Streptavidin and 1% L-glutamine (both Gibco). To monitor cell shape and size and to ensure that the three-dimensional structure of the keratin network remained intact during extraction, we labeled the keratin network using cyan fluorescent protein and yellow fluorescent protein. For this, we transfected cells with eCFPK8WT/eYFPK18WT DNA constructs using the reagent Metafectene (Biontex Laboratories).¹⁵ Prior to experiments, the cells were seeded on round glass slides (Ø 3.5 mm, Fisher Scientific) at a density of 5×10^5 cells per petri dish container (Ø 5cm, Greiner Biotech). After 24 h cells were treated with 1 µg construct DNA and 4 µl Metafectene per 2ml cell culture medium. After an additional 24-h incubation period, the cells were left in culture medium for 12 h. Subsequently, cell samples were synchronized in FCS free medium for at least 12 h. Prior to AFM probing, cells were washed once with FCS free medium.

B. Keratin network extraction and SEM (scanning electron microscopy) sample preparation

The term *in-situ* extracted keratin network is used to describe the structurally intact keratin network after elimination of other cytoskeletal filaments, membranes and soluble cytoplasmic components. The keratin intermediate filament network was extracted following a protocol by Beil *et al.*¹³ After washing cell samples with PBS, the cell membrane was disrupted by 20min treatment with a TritonX solution (1% TritonX-100, 2.2% PEG (35kDa), 50 mM imidazole, 50 mM KCl, 0.5 mM MgCl₂, 0.1 mM EDTA, 1 mM EGTA) at room temperature. Subsequently, the samples were washed twice for 4 min in buffer (50 mM imidazole, 50 mM KCl, 0.5 mM MgCl₂, 0.1 mM EDTA, 1 mM EGTA). In order to remove the remaining actin fibers, the samples were immersed in a gelsolin solution (5 U/ml gelsolin from human plasma, (Sigma), 1 mM CaCl₂, 150 mM KCl, 0.2 mM ATP and 1 mM DTT) at 28 °C for 1 h. Actin fiber staining with phalloidin (Alexa fluor 647 phalloidin, Invitrogen) confirmed a limited actin fiber content in the treated samples. Beil *et al.*¹³ proved the successful extraction of an *in-situ* keratin network using this protocol by subsequent immunogold labeling of the extracted fibers. Finally, the extracted keratin filament networks were washed once with buffer, transferred to PBS and used for indentation testing.

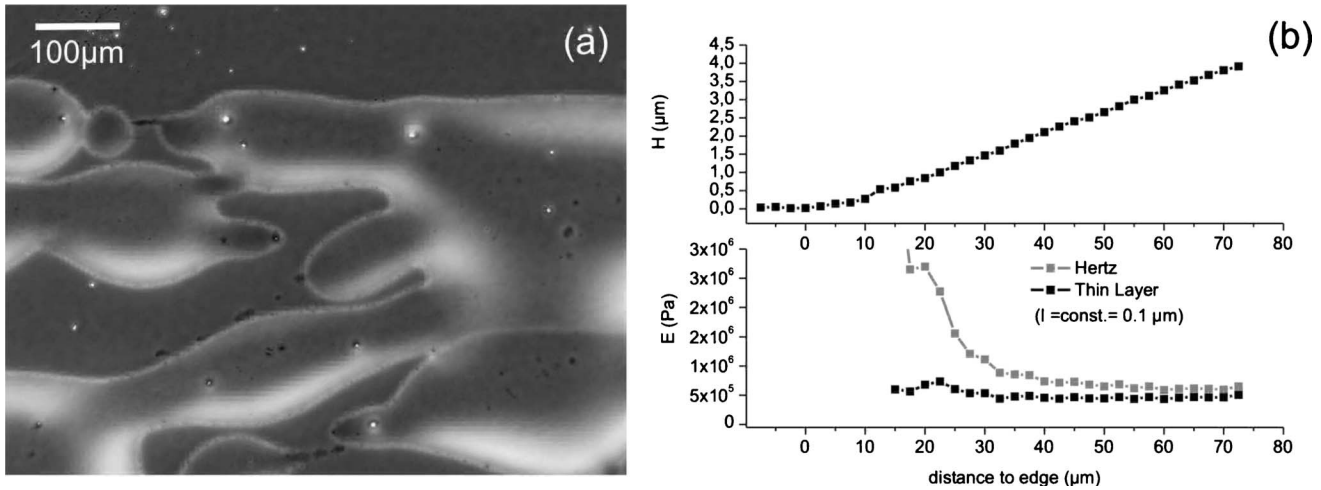


Fig. 1. (a) Phase contrast image of randomly shaped PDMS thin layers of several microns in height. (b) Height H and elastic moduli E plotted over 80 μm from the edge of a thin PDMS layer toward greater height (right). The thin layer corrected model reveals a constant elastic modulus, while the classical Hertz model shows artifacts due to substrate effects at smaller heights, when the indentation depth I is kept constant.

For scanning electron microscopy (SEM) observations the samples must be dried. The extracted keratin filament network was transferred stepwise to 100% ethanol solution (concentration increasing in steps of 20%, 20 min incubation per step) and then critical point dried (CPD 030, BAL-TEC). Afterwards, a layer of 5(+/-2) nm gold was sputtered (Coating System MED 020, BAL-TEC) onto the *in-situ* keratin network to achieve a conductive sample for SEM imaging (Zeiss). Because transfection efficiency is less than 100%, etch-gridded and numbered glass slides (Science Services) were used to keep track of the localization of fluorescence labeled cellular keratin in the SEM image.

C. PDMS thin layer samples and AFM indentation testing

To confirm the applied elastic model for thin layers we performed indentation testing on thin PMDS layers. A single thin hair fiber with a diameter between 50 to 100 μm was dipped in PMDS with a 15:1 base to crosslinker weight ratio (Sylgard 184 Elastomer Kit, Dow Corning). Afterwards, the PDMS was printed on a glass slide in arbitrary patterns, by sliding the fiber over the surface. This resulted in a random PDMS structure of several microns height (see Fig. 1). The polymer samples were cured at 80 $^{\circ}\text{C}$ for two hours and used within 48 h. Prior to indentation experiments, the PDMS samples were oxygen plasma treated for 5s (TePla 100E PS, PVA TePla AG (0.1 mbar O_2 , 100 mW)) to obtain a hydrophilic surface. Indentation measurements were conducted in deionized water at room temperature. Indentation testing on the PDMS thin layers was identical to testing on cells, except for the employment of cantilevers (TL-FM, Nano and More GmbH) with a higher spring constant (approximately 2 N/m).

D. AFM indentation testing on cells/keratin networks and the elastic thin layer model

Indentation testing on living cells and extracted keratin networks was performed using AFM (MFP-3D, Asylum Research). Force-distance curves, which plot the cantilever deflection as a function of the sample height, were acquired from the samples and corrected for baseline drifts. From these curves, force-indentation depth curves (F-I-curves), which describe how much force is needed to indent to a certain sample depth, were deduced by applying Eqs. (1) and (2):

$$F = KD \quad (1)$$

$$I = Z - D. \quad (2)$$

F is the applied force, K is the cantilever spring constant, D is the deflection of the cantilever at contact and Z is the vertical movement of the cantilever during indentation testing. The Z -velocity was held constant at 200 nm/s, thus the measurements can be regarded as quasistatic indentation tests. V-shaped cantilevers (PNP-TR-TL-Au, Nano and More GmbH) with nominal spring constants of 0.02 N/m were utilized for probing. A glass sphere with a diameter of approximately 8 μm (SPI supplies) was attached to the tipless cantilever end via UV curing glue (Loctite 3211, Henkel Technologies) to obtain an indenter with a spherical geometry. Calibration of the cantilever spring constant was performed with the thermal noise method in air atmosphere, prior to probing.¹⁶⁻¹⁸

For data evaluation, the Hertz elastic model for spherical indentation with a correction for thin layers was applied.¹⁹ Equation (3) describes the force-indentation depth (FI) relation for indentation of a thin layer that is bonded to the surface and has an elastic modulus E and height H , utilizing

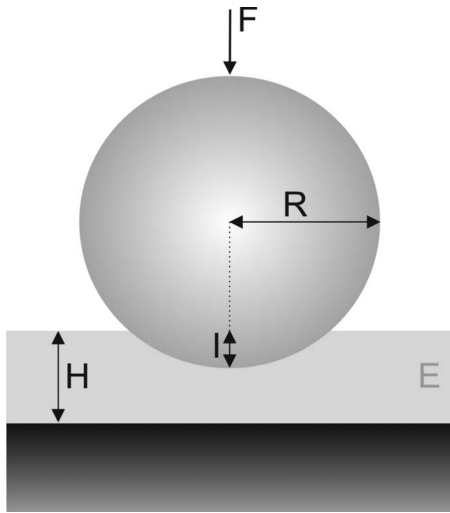


FIG. 2. Sketch of parameters for spherical indentation of a thin elastic layer. F: force, I: indentation depth, R: indenter radius, H: layer height, E: elastic modulus.

a spherical indenter with the radius R (see Fig. 2). The correction is independent of the elastic modulus of the material, but depends on the factor χ (see Eq. (3)).

$$F = \frac{16}{9}ER^{1/2}I^{3/2}[1 + 1.333\chi + 1.283\chi^2 + 0.769\chi^3 + 0.00957\chi^4]; \quad \chi = \frac{[RI]^{1/2}}{H}. \quad (3)$$

For an infinite height or an infinitely small indentation depth, the thin layer model converges to the classical Hertz model (see Eq. (4)).²⁰⁻²²

$$F = \frac{16}{9}ER^{1/2}I^{3/2}. \quad (4)$$

Fits to the data were performed with a custom written Matlab routine (The Mathworks Inc.) applying the least-squares method. The necessary height information from the cells and the keratin networks were calculated from the height difference between contact points on the sample and the glass slide as a reference.

Considering the extensive probing time of whole cell mapping and the symmetry of the keratin intermediate filament network within the cell, we took pointwise measurements in a straight line from the cell edge toward the nucleus. After data processing and fitting, a profile of the elastic modulus across each cell, from cell periphery to the nucleus region, was obtained. In order to compare cells with other cells or with the keratin networks, all elastic profiles are plotted in one graph with the cell width normalized from 0 (nucleus) to 1 (cell edge).

III. RESULTS

We determined the elastic moduli of living pancreatic cancer cells and their extracted keratin intermediate filament

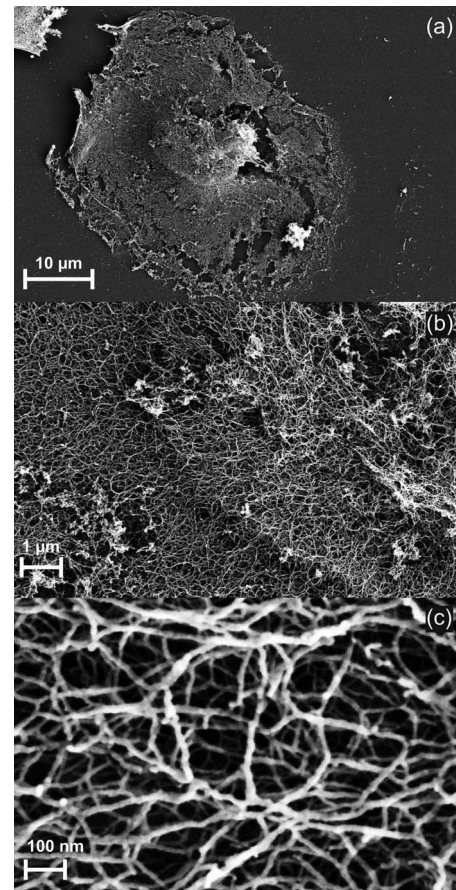


FIG. 3. Scanning Electron Microscope (SEM) images at different magnifications of the extracted *in-situ* keratin intermediate filament network (K8/K18) of a pancreatic cancer cell after detergent treatment. The network mesh density is homogenous throughout the cell, as can be seen in (a) and (b). The measured keratin fiber thickness ranges from 10 to 30 nm and the mesh size varies from approximately 0.006 to 0.06 μm^2 (c).

network utilizing the Atomic Force Microscope (AFM). As the keratin network resists detergent treatment, it is possible to remove all other cellular components, leaving only the *in-situ* keratin network skeleton consisting of keratin variant K8 and K18 (Fig. 3). Imaging of the network during mechanical testing was achieved through fluorescent labeling (Fig. 4).

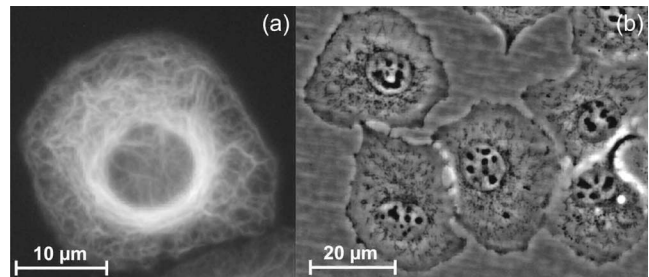


FIG. 4. Fluorescently labeled keratin intermediate filament network of a pancreatic cancer cell (Panc-1) transfected with eCFPK8/eYFPK18 DNA (a) and phase contrast image of Panc-1 cells in culture (b).

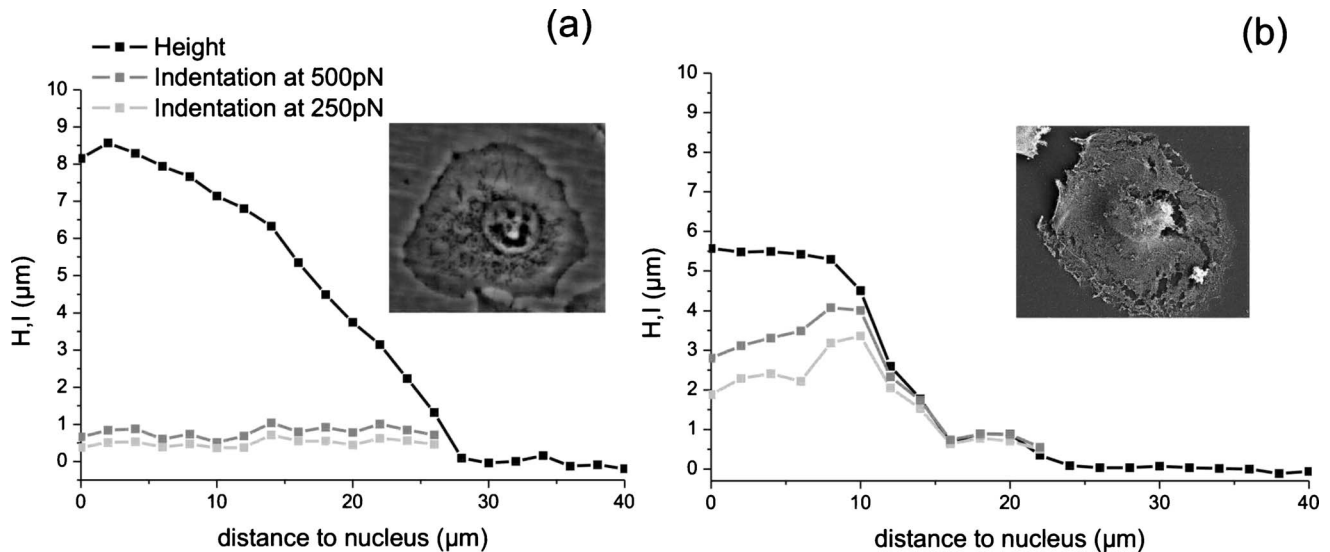


FIG. 5. Comparison of indentation depths I of a living cell (a) and an extracted keratin network sample (b) for constant maximum applied forces of 250 and 500 pN. The keratin sample is indented much deeper than the living cell at identical forces, proving it to be softer. The cell and keratin heights H are plotted as well.

Prior to cell probing, the experimental procedures and the applied elastic material model for thin layers were tested on thin PDMS layers. The sample was indented pointwise in a straight line, starting at the edge of a PDMS thin layer toward increasing height. Both the classical Hertz model (see Eq. (4)) and the thin layer corrected model (see Eq. (3)) were used for analysis of elastic moduli of the PDMS layer at increasing heights with a constant indentation depth (see Fig. 1). As expected for the polymer material, the classical Hertz model reveals a non-constant elastic modulus for different sample heights, while the thin layer model corrects for substrate effects and displays a constant elastic modulus that is independent of the sample height. In addition, the data reveals that the Hertz model elastic modulus depends on the indentation depth (data not shown). This proves the necessity for using a thin layer model for the thin-layered PDMS samples. It also emphasizes the need to correct for substrate effects when performing measurements on samples that are similar in dimension, such as living cells.

Due to time constraints and the symmetrical structure of the keratin networks, we determined the elastic moduli of Panc-1 cells and their keratin networks by pointwise indentation testing in a straight line from the cell edge toward the nucleus rather than whole cell mapping. An initial rough comparison between the mechanical stability of living cells and their extracted keratin network was made by looking at the depth of the indentation for a certain fixed maximum force. Figure 5 shows indentation depths for a living Panc-1 cell and a keratin network sample, after indentation at a maximum force of 250 pN and 500 pN using an indenter of identical shape and size. The extracted keratin was indented deeper at both forces, which proves it to be softer than the cell.

Through detailed analysis of the force indentation curves and application of Eq. (3) on each indentation point, the

elastic profiles of cells and separate keratin network samples were obtained. An example of a single living cell elastic profile is plotted in Fig. 6. For the analysis we used three separate indentation depths (10, 20 and 40% of cell height), so as to avoid indentation depth effects arising from averaging the indentation depth over the contact area between the material and the indenter and from large strains, at which the thin layer model may become invalid. No large strain effects were visible, but for small indentations the choice of the approach point on the sample influenced the elastic moduli data and provoked high oscillations. As a consequence, all further data were analyzed at large indentations (40% height). The homogeneity of the keratin sample was monitored utilizing SEM (Fig. 3). The obtained images reveal an almost homogeneously distributed fiber network and a keratin network mesh size that is 2 to 3 orders of magnitude smaller than the contact area between the indenter and the network during indentation testing. Error analysis of the final elastic moduli revealed a maximum relative resolution of only 20 to 30%, which is due to systematic and statistic data errors, but sufficient for obtaining the following results.

For several samples, a direct graphical comparison of elastic profiles between the *in-situ* keratin (black) and the living cells (red) in Fig. 6 confirms the results obtained from the rough estimation. The elastic moduli of the keratin intermediate filament network are in the order of 10 Pa, while those of the living pancreatic cancer cells range from 100 Pa to 500 Pa. Interestingly, the living cell samples display a high cell-to-cell variation. We also observed that the elastic moduli decrease toward the cell edge, which may be linked to the robustness of the nucleus.²³⁻²⁵ However, the increase is gradual rather than abrupt and no sharp contrast between the nucleus-free cytosolic parts and the nucleus-containing part is visible.

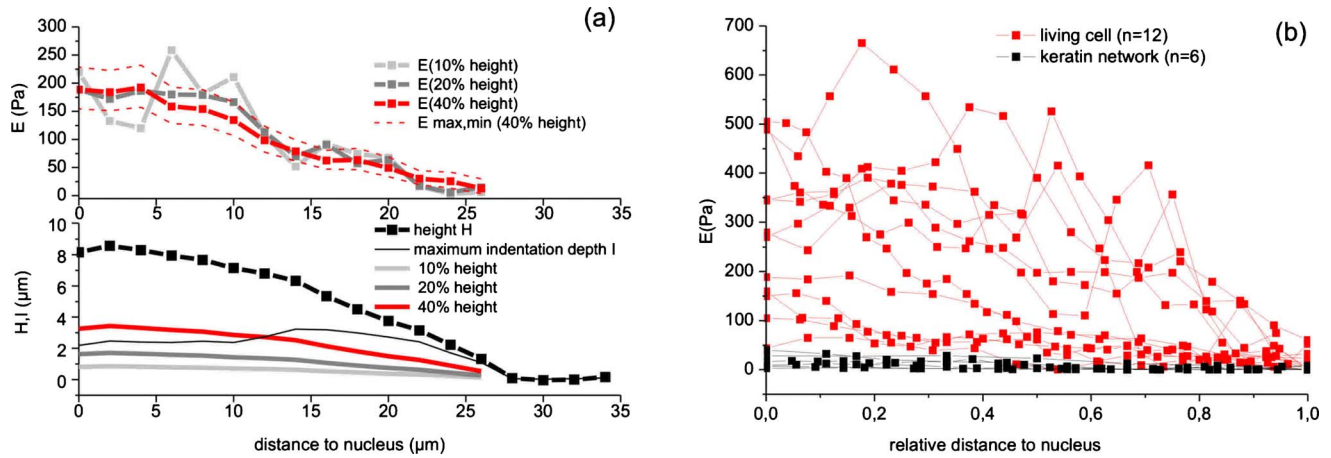


FIG. 6. (Color online) (a) Elastic profile and height profile of a single living cell. The elastic moduli are determined for several indentation depths (10, 20 and 40% of the cell height) applying the thin layer corrected elastic model (see Eq. (3)). (b) Elastic profiles of living cells (red) and extracted keratin networks (black) are compared graphically. The keratin network elastic moduli are only about 2 to 10% of that of the living cell.

IV. DISCUSSION

This work presents a direct comparison between the elastic moduli of living pancreatic cancer cells and their extracted keratin intermediate filament network. By utilizing the same methodology and an identical elastic material model, we avoided comparability issues that can arise when comparing independent measurements. The accurate determination of the mechanical properties of thin films is susceptible to uncertainties arising from both the measurement technique and the applied material models, and very much depends on assumptions concerning the experimental setup. In our experiments, living cells and their keratin intermediate filament networks were approximated as an elastic thin layer for quasistatic and large local deformations during indentation testing with AFM. The elastic moduli of cells and keratin networks were determined using a thin layer elastic model. Further, the suitability of the utilized thin layer model was confirmed with indentation testing on thin polymer (PDMS) layers. It was found that the elastic modulus of extracted keratin networks was only about 2 to 10% of that of living cells (see Fig. 6).

The resolution of quasistatic AFM indentation testing is highly dependable on the cantilever spring constant. Thus, the determination of the spring constant and the calibration of the detection system affected measurements between parts of the cells that differ in their elastic modulus. Assuming no further systematic errors, the elastic moduli of two given points must differ by about 20%–30% to be perceived as different values. In other words, it is probably not possible to resolve elasticity variations due to differences in the keratin intermediate filament network density.

Moreover, additional artifacts are introduced because cells are an inhomogeneous, composite material and have a variable and uneven surface (see Fig. 3–5). Such artifacts could not be quantified here. Cells are dynamic and forever changing and can be activated via processes such as chemical signaling or mechanotransduction. During our experiments, within only a few hours, we were able to observe changes in

cell shape and reorganization of the keratin network (data not shown), like those described previously by other groups.^{26,27} This may partially explain the high cell-to-cell variation found in living cell samples. In addition, cells were polyclonal and not synchronized.

A comparison with previous AFM indentation studies on living cells shows that our results are in good agreement with other published measurements. Li *et al.*²⁸ showed that the elastic moduli of benign and cancerous breast epithelial cells range from 150 to 750 Pa. Limitations of this study are the confinement of cell elasticity measurements to the nucleus-containing area of the cell and the application of the classical Hertz model to small indentation depths. Like our data, these measurements also show high cell-to-cell variability. The only mechanical study performed on *in-situ* extracted keratin networks, thus far, applied microrheological particle tracking to the extracted keratin network of alveolar epithelial cells.¹⁴ These experiments yielded storage moduli at 1 Hz ranging from 95 to 335 dyn/cm², which translates to an elastic modulus of 30 to 110 Pa. These data are in the same order of magnitude as ours and small differences between them may be attributed to the different methodology, and possibly to the different cell types.

The diverse activities of the cytoskeleton depend on three types of protein filaments—actin filaments, microtubules, and intermediate filaments, to which the keratin filamentous network belongs. Being only one of several filament types contributing to cell mechanics, a direct assessment of the impact keratin has on the mechanics of living epithelial cells is difficult, and the role keratin plays has yet to be clearly defined. The keratin network inside the living cell is interwoven with the other cytoskeletal components and the interspaces are filled with high molecular weight molecules and cell organelles. Thus, the inside of the cell can be described as a poroelastic material consisting of a porous, elastic solid (cytoskeleton, organelles, etc.) penetrated by an interstitial fluid (cytosol). In our experiments the keratin elastic modulus was determined in a PBS solution, which does not reflect

the effects of the highly viscous fluid inside the cell. In addition, the possible crosslinking effects with other protein filaments are neglected.

The data presented in this publication take us one step further in understanding the role of the different cytoskeletal elements, by determining the elastic modulus inherent to the cellular K8/K18 keratin network for slow local deformations. The obtained values of approximately 10 Pa represent a lower limit for the mechanical contribution of the keratin network, which can be estimated at roughly 2%–10% inside living pancreatic cancer cells. This seems to indicate that the elastic contribution of the keratin network itself is minor, perhaps even negligible. However, observations have shown a significant change of mechanical values of living cells as a result of a rearrangement of the keratin network.¹³ This suggests that the cytoskeleton is more than just the sum of its parts, and that the crosslinking and intertanglement of the different types of involved filamentous structures is essential in regulating changes in mechanical values in panc-1 cells.

ACKNOWLEDGMENTS

The authors especially acknowledge Professor Subra Suresh (MIT, NSF) who has substantially guided and inspired the research presented here. The authors also acknowledge Dr. Kristen L. Mills, Dr. Iain Dunlop, Dr. Tamas Haraszti and Dr. Nina Grunze for discussion and manuscript improvements. Financial support by the Deutsche Krebshilfe e.V. and the Max Planck Society is highly appreciated. Part of the research leading to these results has received funding from the European Union Seventh Framework Programme (Grant No. FP7/2007-2013) under Grant Agreement No. NMP3-SL-2009-229294 NanoCARD.

¹K. J. Van Vliet, G. Bao, and S. Suresh, *Acta Mater.* **51**, 5881 (2003).

²S. Rammensee, P. A. Janmey, and A. R. Bausch, *Eur. Biophys. J.* **36**, 661 (2007).

³K. E. Kasza, A. C. Rowat, J. Liu, T. E. Angelini, C. P. Brangwynne, G. H.

Koenderink, and D. A. Weitz, *Curr. Opin. Cell Biol.* **19**, 101 (2007).

⁴T. M. Magin, P. Vijayaraj, and R. E. Leube, *Exp. Cell Res.* **313**, 2021 (2007).

⁵E. Fuchs and D. W. Cleveland, *Science* **279**, 514 (1998).

⁶*Intermediate filament cytoskeleton. Methods in Cell Biology*, edited by M. B. Omary and P. A. Coulombe (Elsevier Academic Press, 2004), Vol. 78.

⁷Y.-C. Lin, N. Y. Yao, C. P. Broedersz, H. Herrmann, F. C. MacKintosh, and D. A. Weitz, *Phys. Rev. Lett.* **104**, 058101 (2010).

⁸S. Yamada, D. Wirtz, and P. A. Coulombe, *J. Struct. Biol.* **134**, 44 (2003).

⁹P. A. Janmey, U. Euteneuer, P. Traub, and M. Schliwa, *J. Cell Biol.* **113**, 155 (1991).

¹⁰Y. Luan, O. Lieleg, B. Wagner, and A. R. Bausch, *Biophys. J.* **94**, 688 (2008).

¹¹S. Suresh, *Acta Biomater.* **3**, 413 (2007).

¹²L. Kreplak and D. Fudge, *Bioessays* **29**, 26 (2007).

¹³M. Beil, A. Micoulet, G. von Wichert, S. Paschke, P. Walther, M. B. Omary, P. P. Van Veldhoven, U. Gern, E. Wolff-Hieber, J. Eggermann, J. Waltenberger, G. Adler, J. P. Spatz, and T. Seufferlein, *Nat. Cell Biol.* **5**, 803 (2003).

¹⁴S. Sivaramakrishnan, J. V. DeGiulio, L. Lorand, R. D. Goldman, and K. M. Ridge, *Proc. Natl. Acad. Sci. U.S.A.* **105**, 889 (2008).

¹⁵T. Busch, "Die Rolle von Zytoskelettelementen bei der zellulären Migration und Differenzierung," Ph.D. thesis, University of Ulm (2008).

¹⁶R. Proksch, "Thermal noise spring constant cantilever calibration technique with the MFP-3D AFM," www.asylumresearch.com (June 2009).

¹⁷H.-J. Butt and M. Jaschke, *Nanotechnology* **6**, 1 (1995).

¹⁸J. L. Hutter and J. Bechhoefer, *Rev. Sci. Instrum.* **64**, 1868 (1993).

¹⁹E. K. Dimitriadis, F. Horkay, J. Maresca, B. Kachar, and R. S. Chadwick, *Biophys. J.* **82**, 2798 (2002).

²⁰H. Hertz, *Journal für die reine und angewandte Mathematik* **92**, 156 (1881).

²¹I. N. Sneddon, *Int. J. Eng. Sci.* **3**, 47 (1965).

²²L. D. Landau and E. M. Lifshitz, *Theory of elasticity* (Elsevier Butterworth-Heinemann, 2005).

²³N. Caille, O. Thoumine, Y. Tardy, and J. J. Meister, *J. Biomech.* **35**, 177 (2002).

²⁴F. Guilak, J. R. Tedrow, and R. Burgkart, *Biochem. Biophys. Res. Commun.* **269**, 781 (2000).

²⁵J. D. Pajerowski, K. N. Dahl, F. L. Zong, P. J. Sammak, and D. E. Discher, *Proc. Natl. Acad. Sci. U.S.A.* **104**, 15619 (2007).

²⁶S. Sivaramakrishnan, J. L. Schneider, A. Sitikov, R. D. Goldman, and K. M. Ridge, *Mol. Biol. Cell* **20**, 2755 (2009).

²⁷D. Russell, P. D. Andrews, J. James, and E. B. Lane, *J. Cell Sci.* **117**, 5233 (2004).

²⁸Q. S. Li, G. Y. Lee, C. N. H. Ong, and C. T. Lim, *Biochem. Biophys. Res. Commun.* **374**, 609 (2008).